Layering and Position-Dependent Diffusive Dynamics of Confined Fluids

Jeetain Mittal,[1,*] Thomas M. Truskett,[2,†] Jeffrey R. Errington,[3,‡] and Gerhard Hummer[1,§]
[1]*Laboratory of Chemical Physics, National Institute of Diabetes and Digestive and Kidney Diseases, National Institutes of Health, Bethesda, Maryland 20892-0520, USA*
[2]*Department of Chemical Engineering and Institute for Theoretical Chemistry, The University of Texas at Austin, Austin, Texas 78712-0231, USA*
[3]*Department of Chemical and Biological Engineering, University at Buffalo, The State University of New York, Buffalo, New York 14260-0231, USA*

(Received 4 January 2008; published 11 April 2008)

We study the diffusive dynamics of a hard-sphere fluid confined between parallel smooth hard walls. The position-dependent diffusion coefficient normal to the walls is larger in regions of high local packing density. High density regions also have the largest available volume, consistent with the fast local diffusivity. Indeed, local and global diffusivities as a function of the Widom insertion probability approximately collapse onto a master curve. Parallel and average normal diffusivities are strongly coupled at high densities and deviate from bulk fluid behavior.

DOI: 10.1103/PhysRevLett.100.145901 PACS numbers: 66.10.cg, 61.20.Ja

Beginning with Einstein's theory of Brownian motion, it has been realized that diffusion provides an excellent approximation to the motion of molecules in a bulk liquid for times much longer than intervals between molecular collisions. In molecularly confined systems, the situation is more complicated. On one hand, particle structures emerge that result in a spatially inhomogeneous density profile, and on the other hand, the relaxation time of local density fluctuations may become faster than the time required for particle motions to become "diffusive." Alternatively, long-lived correlations can prevent the system from entering into a diffusive regime altogether, as in single-file transport [1]. Nevertheless, in simulations of partially confined systems such as fluids in two-dimensional (2d) slit pores, diffusion is indeed observed parallel to the infinite confining planes [2,3]. However, the situation is less clear for motions in the perpendicular direction. Even if diffusion were a useful description of the single-particle motions, one would expect the diffusion coefficient to be spatially inhomogeneous. That, combined with the spatially varying density profile and the confining boundaries, essentially eliminates the usual way of estimating diffusion coefficients from the mean-square displacement as a function of time [4]. As a consequence, diffusion in highly confined environments has largely remained unexplored, despite its relevance for micro- and nanofluidic devices [5].

We use a recently proposed propagator-based formalism to estimate the position-dependent diffusion coefficients self-consistently from simulation trajectory data [6]. For diffusion, the propagator (or Green's function) $G(z, \Delta t|z', 0)$ for single-particle displacements along the coordinate z normal to the confining walls is assumed to satisfy the Smoluchowski diffusion equation,

$$\frac{\partial G}{\partial t} = \frac{\partial}{\partial z}\left\{D_{\perp}(z)e^{-\beta F(z)}\frac{\partial}{\partial z}[e^{\beta F(z)}G]\right\}, \qquad (1)$$

with $\beta = 1/k_BT$, k_B Boltzmann's constant, and T the absolute temperature. Spatial discretization of Eq. (1) [7] results in a master equation that describes the single-particle dynamics between neighboring intervals along z. The particle trajectories in the simulations are discretized by assigning positions into bins i along z. We count the numbers N_{ji} that a particle is found in bin i at time τ, and in bin j at time $\tau + t$, irrespective of its location at intervening times, with t the observation (or lag) time and N_{ji} summed over τ. In essence, we then "fit" the diffusion model Eq. (1) to the N_{ji} matrix (which we symmetrize to enforce microscopic time reversibility/detailed balance). This fit is done by determining the likelihood function L for observing N_{ji}. Assuming Eq. (1) for given $D_{\perp}(z_i)$ and $F(z_i)$, L can be written as a product of Green's functions that are expressed in terms of a matrix exponential [6,7]. Here, we use a Bayesian approach with a Jeffreys' prior to infer the $D_{\perp}(z_i)$ and $F(z_i)$ that are most consistent with the observed N_{ji} [6]. Alternatively, we could have maximized the likelihood L. The resulting diffusive model can be validated by comparing its predictions for N_{ji} or $G(z, t'|z', 0)$ to the simulation data for times $t' \neq t$.

Here, we apply this formalism to test whether diffusion provides a quantitative description of the single-particle dynamics perpendicular to the confining planes for a fluid confined in a 2D slit pore. We also explore whether empirical relations between the fluid density and the diffusion coefficient identified for diffusion in bulk and parallel to the walls [3] transfer trivially to perpendicular diffusion.

Hard spheres (HS) confined between hard walls are arguably the most basic model of confinement. Nevertheless, the essential physics of inhomogeneous fluids is captured, such as pronounced local density variations [8] or shifted fluid-solid phase boundaries with respect to bulk [9]. Also, the unambiguous definition of quantities like accessible volume, and rigorous ways to calculate it for hard-sphere fluids [10], can be helpful in elucidating the underlying microscopic mechanisms. Moreover, colloidal systems could be used to test the predictions experimentally [11,12], assuming that at sufficiently high particle densities and at sufficiently long times (compared to the characteristic time τ_c) the differences between our hard-sphere Hamiltonian dynamics and the Brownian dynamics of colloidal particles can be ignored.

We use discontinuous molecular dynamics (DMD) simulations to generate dynamic trajectories for our model system. In DMD, each particle follows a linear trajectory until it collides with another particle or a wall. In a collision, the velocities of colliding particles are changed to conserve energy and momentum [13]. To simplify the notation, dimensionless quantities will be reported, obtained by appropriate combinations of a characteristic length (HS particle diameter σ) and time scale ($\sigma\sqrt{m\beta}$, where m is the particle mass). The packing fraction $\phi = \pi\rho/6$ is defined in terms of the density ρ based on the total (rather than center-accessible) volume [3]. The DMD simulations each involved $N = 3000$ identical HS particles. Periodic boundary conditions were applied in all directions for the bulk fluid and in the x and y directions for the confined fluid. In the confined system, perfectly reflecting, smooth hard walls were placed at $z = \pm H/2$. The transverse self-diffusivity $D_\parallel$ was obtained by fitting the long-time ($t \gg 1$) behavior of the average mean-squared displacement of all the particles to the Einstein relation $\langle \Delta\mathbf{r}^2 \rangle = 4D_\parallel t$, where $\Delta\mathbf{r}^2$ corresponds to the mean-square displacement per particle in the x and y directions.

For calculating $D_\perp(z)$, we use a bin size of 1/10 to divide the space in the z direction. To test the validity of the diffusion model, Eq. (1), we calculate the position-dependent diffusivities as a function of the observation time t. From exponential fits of $D_\perp$ with respect to t at fixed $z = 0$, we find characteristic times $\tau_c < 1$ for $\phi > 0.1$, $H = 3$ and $H = 5$ (not shown). We observe an increase in τ_c with decreasing ϕ, as expected from the decreasing collision frequency. In the following, we report diffusion coefficients calculated for $t = 1$, somewhat underestimating the long-time diffusivity at the lowest densities, $\phi \leq 0.1$.

To test if diffusion captures the dynamics normal to the walls, we compare the long-time propagators $G(z, t|z', 0)$ of the Markovian model to the simulation data. $G(z_j, t|z_i, 0) = N_{ji}/\sum_k N_{ki}$ is the conditional probability in the simulations that a particle starting from bin i at time 0 is found in bin j at a later time t. As shown in Fig. 1 for two different packing fractions and for a pore size $H = 3$, excellent agreement is found between the diffusive model and the DMD data over 6 orders of magnitude in probability.

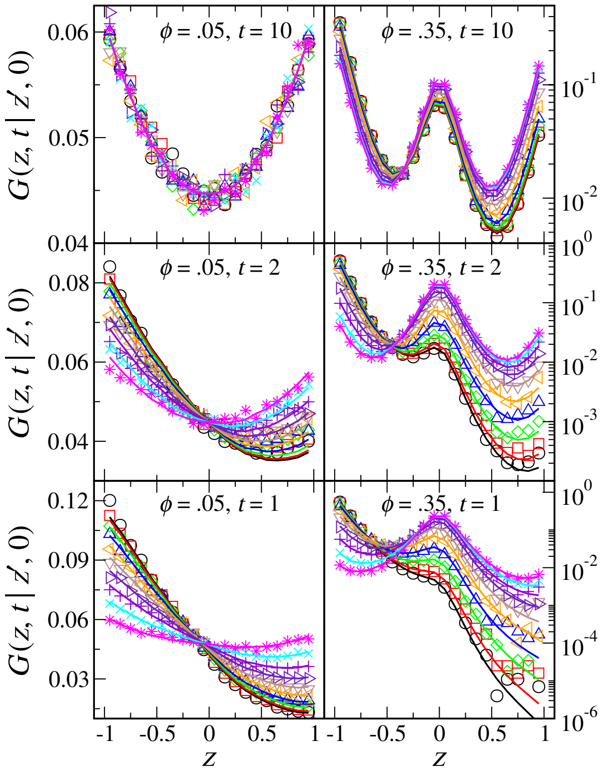

FIG. 1 (color online). The conditional probability $G(z, t|z', 0)$ of observing a particle at a position z at time t if it started at z' at $t = 0$. Results are shown for pore size $H = 3$, packing fractions $\phi = 0.05$ (left) and 0.35 (right), and times $t = 1$, 2, and 10 (bottom to top). The observation time $t = 1$ is used to obtain parameters of the diffusion model Eq. (1) (lines). Simulation results for $G(z, t|z', 0)$ for different z' are shown as symbols, where z' varies from -0.05 to -0.95 (symbol ∘ to *) in intervals of 0.1. (For reference, mean collision frequencies for the bulk hard-sphere fluid are approximately 852 and 7369 for $\phi = 0.05$ and 0.35, respectively.)

Figure 2 compares $D_\perp(z)$ and the local density $\rho(z)$ to explore the effect of wall confinement on the local normal diffusivity. Remarkably, we find that $D_\perp(z)$ is large where $\rho(z)$ is high (except near the walls, where $\rho(z)$ drops sharply). This low diffusivity near the walls is due to the presence of impenetrable reflective wall boundaries, limiting diffusion to one direction. Figure 2 also shows the predictions for $D_\perp(z)$ from hydrodynamic theory in the Oseen approximation, $D_\perp(z) = D_{\mathrm{bulk}}/[f_\perp(z + H/2) + f_\perp(H/2 - z) - 1]$, where $f_\perp(h)$ is the correction factor to the Stokes friction for a spherical particle moving perpendicular to a planar free surface [14] and the bulk diffusivity D_{bulk} is calculated at the average pore density ρ. A similar theory successfully described the in-plane motion of a colloidal particle between two walls [15]. Here, we find that at packing fractions $\phi > 0.15$ the hydrodynamic theory is remarkably accurate, quantitatively reproducing the plateau of $D_\perp(z)$ near the center and qualitatively the drop at the walls. However, as expected, the $D_\perp(z)$ from hydrodynamics is not structured, lacking information about the molecular correlations and layering of the fluid.

At first sight, the positive correlation between high local density and faster local diffusion may appear counterintuitive as diffusivity for bulk fluids usually decreases with

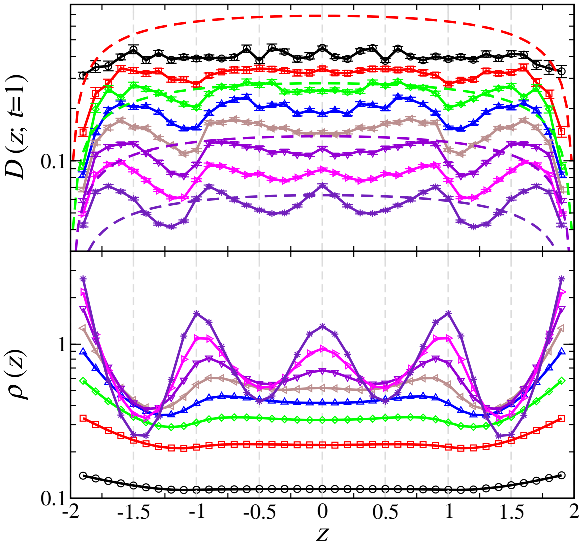

FIG. 2 (color online). Local normal diffusivity $D_\perp(z)$ and density profile $\rho(z)$ versus position in the z direction for a pore size $H = 5$ and packing fractions $\phi = 0.05$, 0.10, 0.15, 0.20, 0.25, 0.30, 0.35, and 0.40 (top to bottom for $D_\perp(z)$ and bottom to top for $\rho(z)$). The predictions for $D_\perp(z)$ from hydrodynamic theory (see text) are also shown as dashed lines for $\phi = 0.10$, 0.20, 0.30, and 0.40. The local free energy $F(z)$ (not shown) constructed from the propagators is consistent with the equilibrium density profile, $F(z) = -k_B T \ln\rho(z)$ up to an arbitrary constant.

increasing density. To understand this unexpected behavior for inhomogeneous fluids, we turn our attention to the physics of layer formation in the confined environments. The confined fluid is structured normal to the walls and forms layers to maximize its entropy [16]. Similarly, the homogeneous hard-sphere fluid crystallizes at high enough densities to maximize entropy [17,18]. We note that the activity $\xi = \exp(\beta\mu)/\lambda^3$ of an equilibrated confined system is spatially invariant, even though the density is not (where μ is the chemical potential and λ is the thermal wavelength). Also, for a hard-sphere fluid, $\xi = \rho(z)/P_0(z)$ [10], which means that the local insertion probability $P_0(z)$ (or local available volume [19]) is directly proportional to the density $\rho(z)$. In other words, the idea that dense "layers" actually have more available space than the gaps between them is a consequence of this simple and exact relationship derived more than 40 years ago by Widom [10]. If we think of diffusion as particles probing their surroundings for space, then P_0 should indeed be a relevant quantity. A "prediction" would then be that $D_\perp(z)$ should approximately collapse as a function of $P_0(z)$.

To test this prediction, we either need the particle insertion probability P_0 as a function of z or the activity ξ as a function of pore size H and average pore density along with the density profile $\rho(z)$. Using the particle insertion method can be very time consuming and even practically limited at high densities. Instead, we use grand canonical transition matrix Monte Carlo (GC-TMMC) simulations to evaluate the functional relationship between the activity ξ and the average pore density ρ for a given H. The details of the GC-TMMC method are documented in [20] and the specific implementation details are as in [21].

In Fig. 3, we show $D_\perp$ versus P_0 over a wide density range ($\phi = 0.05$–0.4) for two pore sizes ($H = 3$ and 5). The relationship for the bulk hard-sphere fluid and for the transverse diffusivity are also shown on the same plot. We find that the $D_\perp$ data (closed and empty symbols) approximately collapse to a power law form which in turn is very similar to the bulk relationship shown by the solid line. Note that right next to the wall, this relation does not hold (marked by the shaded area in Fig. 3). However, this is expected because at the wall particles can only diffuse in one direction (i.e., away from the wall). Overall, the approximate collapse in Fig. 3 supports the idea that the local available volume, probed by the insertion probability, is indeed a relevant quantity for diffusion.

We also notice in Fig. 3 that the local normal diffusivity is lower than the corresponding bulk value, when compared at the same value of P_0. This is expected because the presence of the walls directly hinders normal diffusivity in ways that are not reflected by the local available space. Of course, this becomes a relatively small effect at high ρ and is reflected in Fig. 3 by a convergence of the $D_\perp$, $D_\parallel$, and bulk diffusivity at low P_0. The reason for the slightly higher $D_\parallel$ stems from a higher chemical potential required to achieve the average pore density equal to the bulk and has been discussed in detail elsewhere [21].

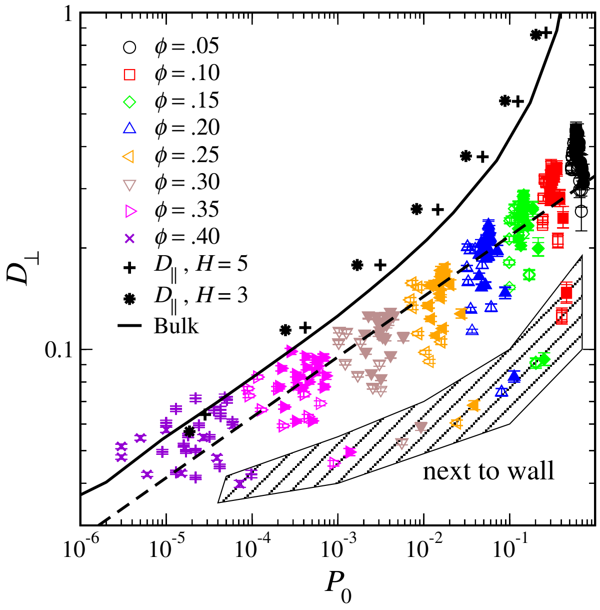

FIG. 3 (color online). Local normal diffusivity $D_\perp(z)$ at different packing fractions ϕ as a function of the local available volume, measured by the local insertion probability $P_0(z)$. Filled and empty symbols correspond to $H = 5$ and 3, respectively. Data for bulk are shown by a solid line. The dashed line is a power law fit to the $D_\perp$ data. The average transverse diffusivity $D_\parallel$ is also shown for reference.

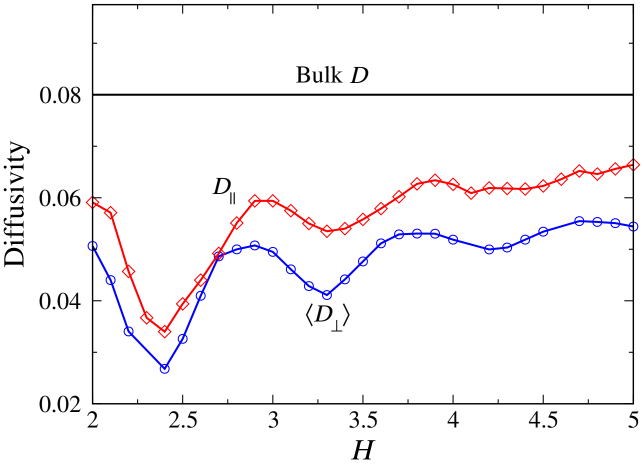

FIG. 4 (color online). The average normal (blue circles) and transverse (red diamonds) diffusivity versus the pore size H is shown for a packing fraction of $\phi = 0.40$. The corresponding bulk diffusivity is shown as a solid horizontal line.

We can also use our formalism to explore the coupling between diffusion in the transverse and normal directions. In an earlier study [21], it was observed that $D_{\|}$ of the confined HS fluid shows pronounced negative deviations from bulk fluid behavior for relatively high density (e.g., $\phi = 0.4$) and small pore widths ($H < 3$). These deviations have an oscillatory dependence on H with slower diffusion occurring for pore sizes that do not naturally accommodate an integer number of particle layers in the density profile. Based on such information, it was hypothesized [21] that one might also expect a coupling between single-particle dynamics in directions parallel and normal to the confining walls. Here, we test this idea by calculating the average normal diffusivity $\langle D_{\perp}\rangle = \int_0^{H/2} D_{\perp}\rho dz / \int_0^{H/2} \rho dz$ and comparing it to $D_{\|}$ in Fig. 4. The slightly higher diffusivity in plane than perpendicular reflects the anisotropic, layered molecular structure.

As shown in Fig. 4, the H-dependent oscillations of $\langle D_{\perp}\rangle$ closely track those of $D_{\|}$. Remarkably, the oscillations in $D_{\|}$ and $\langle D_{\perp}\rangle$ as a function of H follow the pore-width dependence of the phase boundary $\phi_f(H)$ between the confined solid and fluid HS system [9], and also the excess entropy per particle [21]. These correlations illustrate the connection between dynamic and thermodynamic properties arising from packing frustration. In particular, these results provide strong support for the picture that confinement-induced frustration affects diffusive particle motions in both principal directions.

J. M. wishes to thank Jyoti Seth (University of Texas at Austin) for her careful reading of an early draft. This research was supported in part by the Intramural Research Program of the NIH, NIDDK. T. M. T. and J. R. E. acknowledge the financial support of the National Science Foundation under Grants No. CTS-0448721 and No. CTS-028772, respectively. T. M. T. also acknowledges the support of the David and Lucile Packard Foundation and the Alfred P. Sloan Foundation. The Texas Advanced Computing Center (TACC) and University at Buffalo Center for Computational Research provided computational resources for this study. A portion of this study utilized the high-performance computational capabilities of the Biowulf PC/Linux cluster at the National Institutes of Health, Bethesda, MD (http://biowulf.nih.gov).

[*] jeetain@helix.nih.gov
[†] truskett@che.utexas.edu
[‡] jerring@buffalo.edu
[§] hummer@helix.nih.gov

[1] K. K. Mon, J. K. Percus, and J. Yan, Mol. Simul. **29**, 721 (2003).
[2] J. J. Magda, M. V. Tirrell, and H. T. Davis, J. Chem. Phys. **83**, 1888 (1985).
[3] J. Mittal, J. R. Errington, and T. M. Truskett, Phys. Rev. Lett. **96**, 177804 (2006).
[4] P. Liu, E. Harder, and B. J. Berne, J. Phys. Chem. B **108**, 6595 (2004).
[5] L. Bocquet and J. L. Barrat, Soft Matter **3**, 685 (2007).
[6] G. Hummer, New J. Phys. **7**, 34 (2005); S. Sriraman, I. G. Kevrekidis, and G. Hummer, J. Phys. Chem. B **109**, 6479 (2005).
[7] D. J. Bicout and A. Szabo, J. Chem. Phys. **109**, 2325 (1998).
[8] H. T. Davis, *Statistical Mechanics of Phases, Interfaces, and Thin Films* (Wiley-VCH, New York, 1996).
[9] A. Fortini and M. Dijkstra, J. Phys. Condens. Matter **18**, L371 (2006).
[10] B. Widom, J. Chem. Phys. **39**, 2808 (1963).
[11] E. R. Weeks, J. C. Crocker, A. C. Levitt, A. Schofield, and D. A. Weitz, Science **287**, 627 (2000).
[12] C. R. Nugent, K. V. Edmond, H. N. Patel, and E. R. Weeks, Phys. Rev. Lett. **99**, 025702 (2007).
[13] D. C. Rapaport, *The Art of Molecular Dynamics Simulations* (Cambridge University Press, Cambridge, England, 2004).
[14] J. Happel and H. Brenner, Low Reynolds Number Hydrodynamics (Prentice-Hall, Englewood Cliffs, 1965).
[15] B. Lin, J. Yu, and S. A. Rice, Phys. Rev. E **62**, 3909 (2000); E. R. Dufresne, D. Altman, and D. G. Grier, Europhys. Lett. **53**, 264 (2001).
[16] R. Kjellander and S. Sarman, J. Chem. Soc., Faraday Trans. **87**, 1869 (1991).
[17] B. J. Alder and T. E. Wainwright, Phys. Rev. **127**, 359 (1962).
[18] W. G. Hoover and F. H. Ree, J. Chem. Phys. **49**, 3609 (1968).
[19] S. Sastry, T. M. Truskett, P. G. Debenedetti, S. Torquato, and F. H. Stillinger, Mol. Phys. **95**, 289 (1998).
[20] J. R. Errington, J. Chem. Phys. **118**, 9915 (2003).
[21] J. Mittal, J. R. Errington, and T. M. Truskett, J. Chem. Phys. **127**, 154513 (2007).